Cloud Publications
International Journal of Advanced Remote Sensing and GIS
2016, Volume 5, Issue 6, pp. 1795-1812
ISSN 2320 - 0243, Crossref: 10.23953/cloud.ijarsg.61

Research Article | Open Access

Population Estimation in an Urban Area with Remote Sensing and Geographical Information Systems

Dimitris Kaimaris[1] and Petros Patias[2]

[1]School of Spatial Planning and Development (Eng.) Aristotle University of Thessaloniki, Greece
[2]School of Rural and Surveying Engineering, Aristotle University of Thessaloniki, Greece

Publication Date: 27 June 2016

DOI: https://doi.org/10.23953/cloud.ijarsg.61

Abstract Population estimation with questionnaires and demographic models is time consuming and usually accompanied by high costs. Geoinformation tools constitute key tools towards the solution of this problem, and, therefore, studies have started to emerge in the early 70s. In this paper a brief reference to the methods of population estimation, which are based totally or in combination with statistical analysis methods on products of Remote Sensing and their processing with GIS is cited. Afterwards, the capability of stereoscopic satellite images of high spatial resolution for the determining of the height of buildings and the performance of their plans, which are essential data for the estimation of the population of each building is highlighted. The study area is the municipality of Thessaloniki (Northern Greece, Region of Central Macedonia), and the estimation accuracy of the population reaches 97.06%.
Keywords *Population Estimation; Remote Sensing; Ikonos-2; DSM; DTM; GIS*

1. Introduction

In Greece, the responsible principal for the documentation of the population census is the Greek Statistical Authority (ELSTAT). The methodology is costly, time consuming and relies on processing of census/residences questionnaires (method of interview within the respondents residence), in combination with their statistical study and processing.

The last census took place in Greece in 2011, and the preceding one in 2001 (short-term analysis). On the internet, freely available data for 2001 are provided at municipal districts' level (large spatial areas within municipalities); while for 2011 they are provided only at the municipal level (even larger territorial areas, since municipalities consist of districts or sections). Data at building level do not exist at all, and free data at blocks' level are not provided. However, apart from the demographic models for population estimation, Remote Sensing and Geographic Information Systems (GIS) are also utilized for this purpose.

The benefits of population estimation, beyond urban and regional planning, are obvious and have been described in many studies (Smith and Mandell, 1984; Benn, 1995; Smith et al., 2002; Liu, 2003;

Qiu et al., 2003; Lang et al., 2010; Deng et al., 2010). The estimation of daytime population, which is required, for example, in the case of constructing an evacuation plan of a city during rush hours, is currently difficult to tools of geoinformatics. The first attempts to estimate the residential population by means of Remote Sensing (and with the help of Geographical Information Systems, GIS) started in the 70s. The methodologies are distinguished, according to Wu et al. (2005), in areal interpolation methods (with subcategories auxiliary information are used) and statistical modeling methods (with subcategories based on the relationship between the population with urban areas, land uses, characteristics of satellite imagery and other natural or socio-economic characteristics).

An improvement of areal interpolation methods is the implementation of Pycnophylactic interpolation, dasymetric-mapping method or/and a combination of both (Langford, 2006; Mennis and Hultgren, 2006; Kim and Yao, 2010).

As far as statistical modeling methods are concerned, ordinary least squares (OLS) regression is the most commonly used method, while geographically weighted regression (GWR) provides better results (Harvey, 2002; Qiu et al., 2003; Wu and Murray, 2007; Dong et al., 2010; Deng et al., 2010).

The methodologies that include processing (eg classification) of satellite images for the exportation of dwelling units (and other coverages) give better population estimation results (Lo, 1995; Harvey, 2002; Wu et al., 2005; Li and Weng, 2005; Bagan and Yamagata, 2015). Nighttime images from the Defense Meteorological Satellite Program's Operational Linescan System (DMSP OLS) and the International Space Station (ISS) have been combined with census population data, and by the use of simple linear regression methods it has been proved that there is a correlation between the intensity of pixel brightness and the population data, but the assessment of both the urban population and its density is not satisfactory. Progress is expected due to their spatial resolution improvement beyond today's 50 m (Sutton, 1997; 2003; Anderson et al., 2010). In conclusion, through the visual interpretation of images (Lo, 1986; Yagoub, 2006) for the detection of dwelling units, the insertion of remote sensing products in predictive mathematical models (Al-Garni, 1995; Qiu et al., 2003), the correlation of specific spectral regions with urban space and, therefore, the population (Iisaka and Hegedus, 1982; Lo, 1995; Harvey, 2002; Li and Weng, 2005; Joseph et al., 2012; Zhu et al., 2015), and the statistical analysis and combination of demographic data with the Earth's surface coverages (Qiu et al., 2003; Lo, 2008; Avelar et al., 2009; Dong et al., 2010; Deng et al., 2010; Mao et al., 2012; Zhu et al., 2015), Remote Sensing is a powerful tool on the supply of data for assessment procedures on residential population (Tatem et al., 2007; Doll, 2008; Chand et al., 2009; Azar et. al., 2010). The improvement of the spatial resolution of (daytime) satellite images (Yagoub, 2006; Lang et al., 2010), the use of object-orientated classification (Lang, 2010; Silvan-Cardenas et al., 2010) for land coverages exportation, and the utilization of Lidar data (Lu et al., 2006; Wu et al., 2008; Xie et al., 2008; Aubrecht et al., 2009; Chen et al., 2009; Silvan-Cardenas et al., 2010; Lu et al., 2010; Dong et al., 2010), which enable both the identification and rendering of the outline of the buildings and the correlation of their height with the population have helped towards this direction.

However, the supply of Lidar data is accompanied by high costs. It would be advantageous to use stereoscopic satellite images, which could provide a twofold benefit as it would allow the production of the necessary DSM (Digital Surfaces Model) for the extraction of building heights and the differentiation of buildings through image classification. This study moves towards this direction (use of stereoscopic images), where an effort is made to assess the population with the urban limits of the Municipality of Thessaloniki (Greece, Figure 1). The spatial processing of satellite images aims at the identification of the location and height of each building, information which will be used for the population assessment with the use of GIS. Moreover, the population census information will be used to verify the final result.

2. Study Area

The prefecture of Thessaloniki (Central Macedonia, Greece, Figure 1 and 2) has a population of 1,110,312 residents (census of ELSTAT 2011), essentially concentrating 9.4% of the Country's population. The Municipality of Thessaloniki (Figure 2), which will be the study area, is the second largest municipality of Greece. The former plan "Kapodistrias" (1997-2010, a plan for the optimization of public administration at local government level) divided the municipality in 5 municipal districts (Figure 3). The existing plan "Kallikratis" (2011 until present), on the one hand, merged municipalities so as to create larger administrative entities and, on the other hand, renamed from municipal districts to municipal units. The population estimation of the municipality of Thessaloniki through remote sensing and GIS cannot utilize population data from the municipal section of the historical center of the city (identified with the municipal district 1 in Figure 3), and this is due to the pure commercial use of the buildings. In fact, only a small percentage of the buildings in the historical center appear to be residential. The last population census (ELSTAT) of the historical center (and all municipal districts of the country) was conducted in 2001. In the new 2011 census, population information appears only at municipality level and not at municipality unit level. Therefore, comparative data for the municipality of Thessaloniki, deducting the population of the historical center, can be retrieved only for the census of 2001. Specifically, according to the census of 2001, the municipality of Thessaloniki has a population of 363,987 and the municipal district of the historical center (1 in Figure 3) has a population of 53,017. Therefore, the population of the municipal districts 2 to 5 (Figure 3) of the municipality of Thessaloniki is 310,970.

Figure 1: *Thessaloniki's position in Greece*

Figure 2: *With dotted line are the boundaries of the Region of Central Macedonia, with green line the boundary of the prefecture of Thessaloniki and with red line the municipality of Thessaloniki*

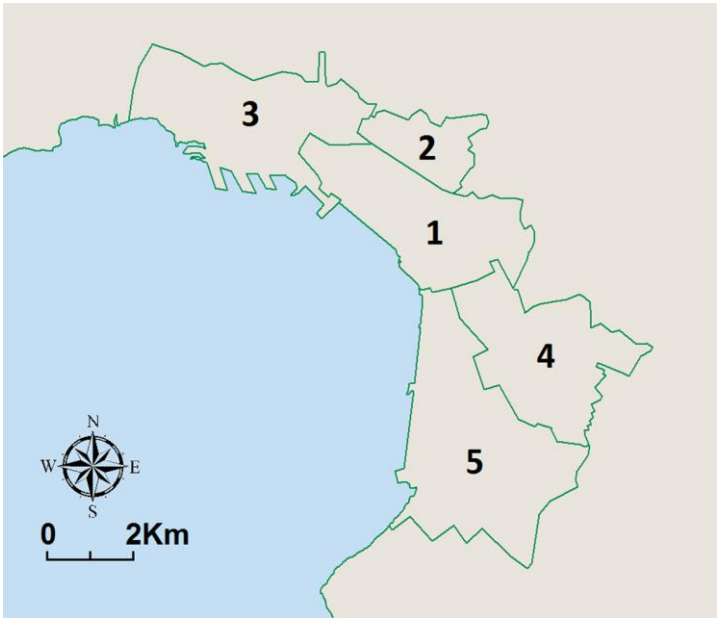

Figure 3: *The municipal districts 1 to 5 of Thessaloniki*

Subsequently in this study satellite images before 2011 will be used for the exportation of suitable products, which after their insertion and processing in GIS will allow the population estimation of the municipality of Thessaloniki (without the historic center). The result will be compared with the population of 310,970, which was mentioned at the end of the previous paragraph.

3. Methodology of Population Estimation

To begin with, the empirical equation (Eq.1) which was created for the population estimation of each building is presented, and afterwards the way that Remote Sensing and GIS allow for the export and processing of the necessary data.

$$\text{Building population} = \frac{(NFB - A) * E_{\text{building}}}{E_{\text{person}}} \quad (1)$$

Where NFB = Number of Floors of the Building = $\frac{H_{\text{building, max}} - H_{\text{building, min}}}{H_{\text{floor}}}$,

$H_{\text{building, max}}$ the highest altitude of the building,

$H_{\text{building, min}}$ the lowest altitude of the building (building's base altitude),

H_{floor} the nominal height of each floor in m,

A the reduction coefficient for the building floors (Table 1),

E_{building} the area of the building plot, and

E_{person} the average area per capita of each property.

Table 1: *Value of the number of floors of the building (NFB) and coefficient A*

NFB Value	A Value	Justification
1	1	The category is about ground floor buildings that are ancillary municipal structures, retail use constructions, etc. With value NFB=1 and by the coefficient A = 1 in the building, no population is attached (Eq. 1).
2	1	One of the two floors is the roof of the property. With value NFB=1 and by the coefficient A = 1 in the building, population is attached only to the ground floor (Eq. 1).
>2	2	The top floor of the building is the roof that contains the installation and the mechanism of the lift or is the floor of the lifting mechanism installation. The ground floor in the majority of buildings in the municipality of Thessaloniki, in case of NFB> 2, is used for retail, for the parking, etc., and not as a residence. With value NFB>2 and by the coefficient A = 2, the building's ground floor and top floor are excluded from the estimate of the population (Eq. 1).

Coefficient A values in Table 1 are adjusted each time in each study area, according to construction rationale of buildings and the use of the floors. Random selection of A values brings population results that have nothing to do with reality.

In equation (1) $H_{\text{floor}} = 3.5m$, and according to Greek urban planning standards (FEK 285/5 March 2004, states that "the accepted indicator, under the applied program for sustainable development, for the first residence is considered to vary between 28-45 sqm / person") the average area per capita is $E_{\text{person}} = 36.5$ sqm. So the equation (1) transforms in:

$$\text{Building population} = \frac{(\frac{H_{\text{building, max}} - H_{\text{building, min}}}{3.5} - A) * E_{\text{building}}}{36.5} \quad (2)$$

Through the classification of satellite images the identification and the extraction of each building plan of the city can be conducted. The result will be the calculation of the area of each building plan (E_{building}), while through the processing of stereoscopic satellite images the DSM (Digital Surface Model) and DTM (Digital Terrain Model) of the city will be determined. These products, after their insertion in GIS will allow for the calculation of the maximum (from DSM) and the minimum altitude

(from DTM) of each building. Then utilizing equation (2) and Table 1 (A coefficient), the processing of the population estimation of each building can be conducted (Figure 4).

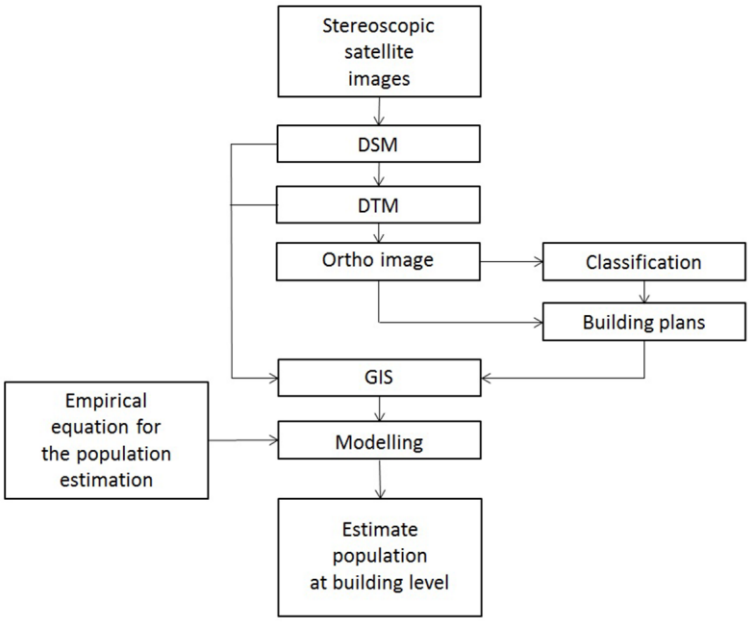

Figure 4: *The flow chart of the operations carried out for population estimation*

4. Satellite Data

Stereoscopic satellite data before 2011 and up to 2001 were searched. The used data are presented in Table 2 and Figure 5.

Table 2: *Stereoscopic satellite images*

Type	Acquisition Date/Time	Bands	Nominal Collection Elevation	Spatial resolution
Ikonos-2	2008-07-18 09:23 GMT	RGBNIR	69.24175 degrees	1 m
Ikonos-2	2008-07-18 09:23 GMT	RGBNIR	74.73024 degrees	1 m

5. Processing of Satellite Images

5.1. Production of DSM, DTM and Ortho Satellite Images

For the satellite triangulation, fractional polynomials (RPC) of satellite images were used, 12 GCPs (Ground Control Points) and 13 CPs (Check Points, Figure 6), which were measured in the field with horizontal and vertical accuracy of 10 cm and 20 cm respectively. The utilized software was LPS 2011® (a photogrammetric suite of Erdas Imagine 2011®).

According to the results of the satellite triangulation, the marking precision in satellite images is:

$$\sigma_o = 0.305\,pixel = 0.3m \text{ , as } 1pixel = 1m .$$

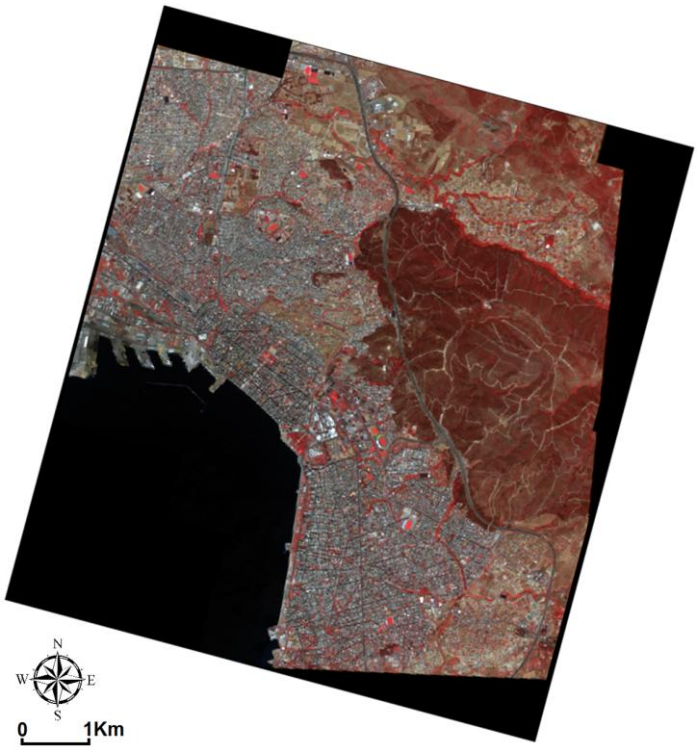

Figure 5: *The satellite image of stereo pair Ikonos-2, RGBNIR*

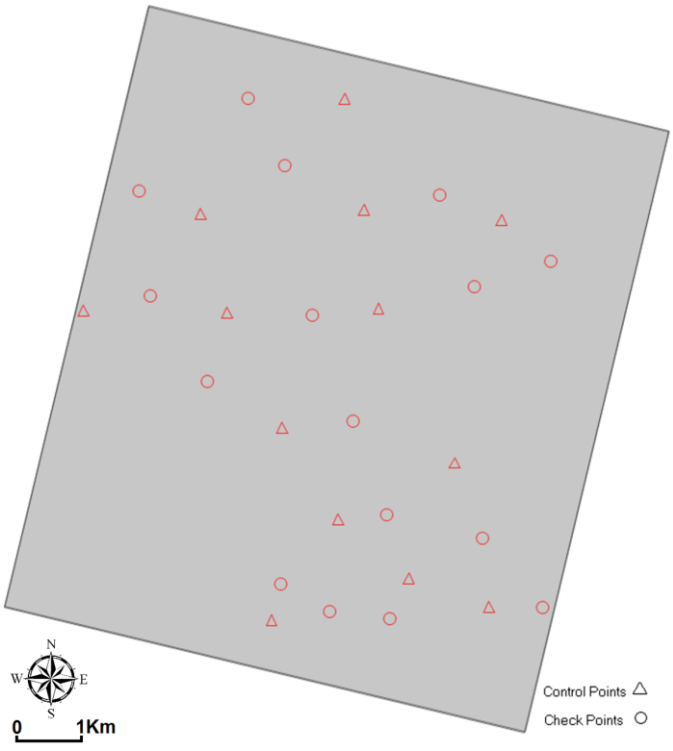

Figure 6: *Distribution of GCPs and CPs in the stereoscopic images*

For Check Points (CPs) the horizontal and vertical standard deviation is:

$$\sigma_{XY,triang.} = \sqrt{0.851^2 + 1.041^2} = 1.34m$$

and

$$\sigma_{Z,triang.} = \sigma_z = 1.36m$$

Afterwards, during the production of DSM (Figure 7) Table 3 was calculated for the entire usable area of stereo images.

Table 3: *Accuracy Information: General Mass Point Quality*

Excellent	56.86 %
Good	31.30 %
Fair	0.00 %
Isolated	0.00 %
Suspicious	11.84 %

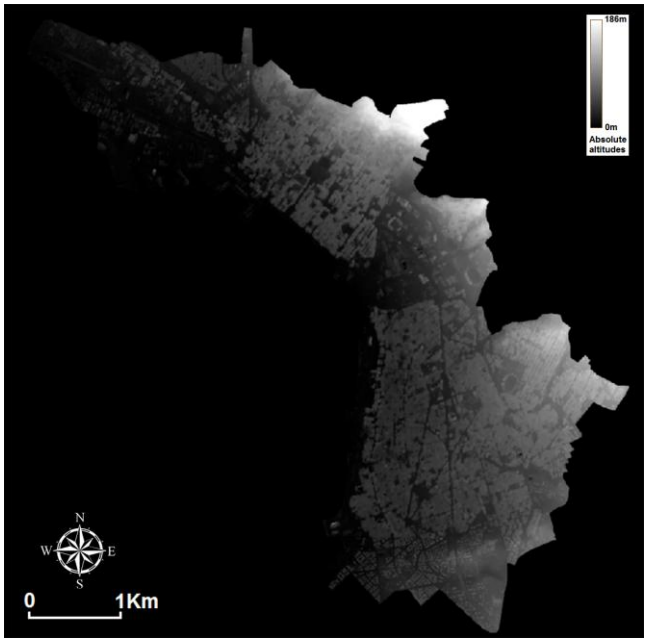

Figure 7: *The DSM of the Municipality of Thessaloniki, Greece*

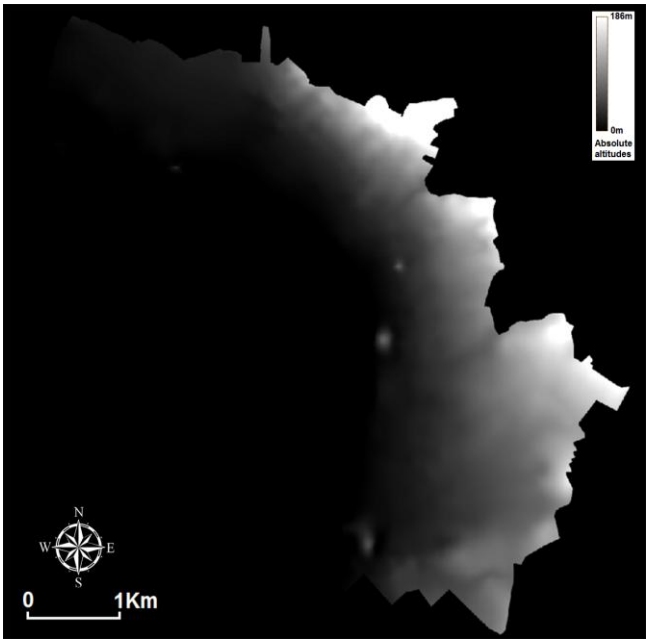

Figure 8: *The DTM of the Municipality of Thessaloniki, Greece*

The assessment of the necessary for this research variation of altitude differences follows.
The assessment of altitude differences is retrieved from the equation:

$$\hat{\Delta}z = \frac{\sum_{i=1}^{n} \delta z_i}{n} = \frac{\sum_{i=1}^{n} \left| z_{DSM,i} - z_{CP,i} \right|}{n}$$

where δz_i represents the differences in the altitudes of check points within the calculated DSM and the field, $z_{DSM,i}$ the altitudes of check points within the calculated DSM , $z_{CP,i}$ the altitudes of check points measured in the field, and n the number of observations.

Thus: $\hat{\Delta}z = 1.3m$

For the assessment of the standard deviation of altitude differences the following equation is used:

$$\hat{\sigma} = \sqrt{\frac{1}{n-1}\sum_{i=1}^{n}\left(\delta z_i - \hat{\Delta}z\right)^2} = \sqrt{\frac{1}{n-1}\sum_{i=1}^{n}\left(\left|z_{DSM,i} - z_{CP,i}\right|\right) - \hat{\Delta}z)^2}$$

and eventually results in:

$$\hat{\sigma} = 0.9m$$

However, it is necessary that: $\hat{\sigma} \leq \sigma_{DSM} = 2\frac{h}{b}\sigma_o$

Where σ_{DSM} is the expected accuracy of the generated DSM , h the vertical distance of the stereo pair from the stereoscopic central point on the ground, and b the base of the stereo pair.

For a calculation of the ratio $\frac{h}{b}$ angles of the satellite images acquisition (Nominal Collection Elevation) are used. Table 2 provides the relative information:

A_1 =69.24175 degrees and A_2 =74.73024 degrees.

Angle A_3 (Figure 9) is derived as follows:

$$A_3 = 180^o - (A_1 + A_2) = 36.02801 \deg rees$$

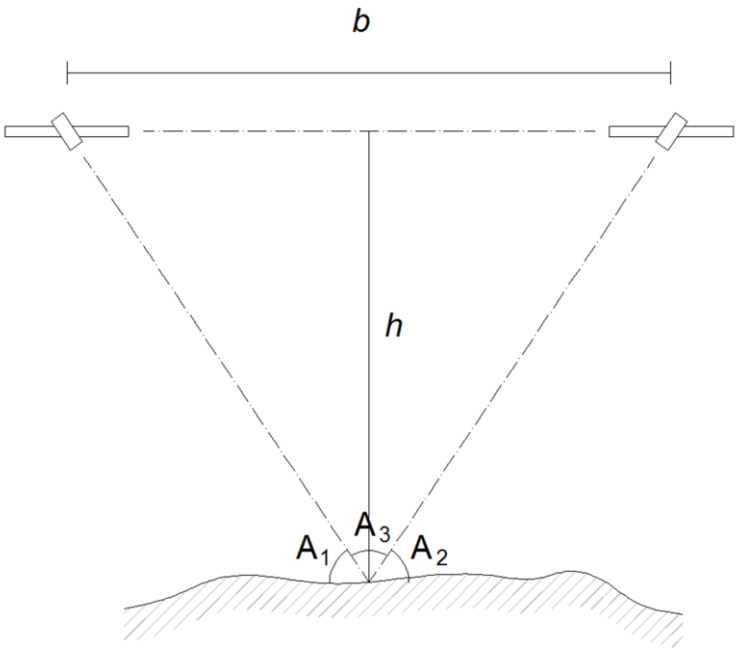

Figure 9: *The acquisition angles, the base of the stereo pair and the vertical distance of the stereo pair from the main stent point*

The base of the stereo pair is the basis of a theoretical isosceles triangle (due to long distances the two sides of the triangle are considered equal), and thus:

$$\tan\frac{A_3}{2}=\frac{b/2}{h}\Rightarrow\frac{h}{b}=\frac{1}{2\tan\frac{A_3}{2}}$$

Where eventually is calculated that: $\frac{h}{b}=\frac{1}{0.65}$

Replacing the calculated values it becomes clear that the test is valid, as:

$$\hat{\sigma}\leq\sigma_{DSM}=2\frac{h}{b}\sigma_o=2\frac{1}{0.65}0.305=0.94m\Rightarrow 0.92m<0.94m$$

There after the assessment of the standard deviation of the estimated height differences (standard error of height differences) is calculated:

$$\hat{\sigma}_{\hat{\Delta}z}=\frac{\hat{\sigma}}{\sqrt{n}}$$

$$\hat{\sigma}_{\hat{\Delta}z}=0.23m$$

The confidence interval for the actual height differences Δz is:

$$\hat{\Delta}z-\hat{\sigma}_{\hat{\Delta}z}t_{n-1}^{\alpha/2}<\Delta z\leq\hat{\Delta}z+\hat{\sigma}_{\hat{\Delta}z}t_{n-1}^{\alpha/2}$$

In the case of normal distribution, and especially in the case of t distribution. That calculation was A confidence factor of $1-\alpha=0.90$ (probability 90%) was set for the calculations, i.e. $\frac{\alpha}{2}=0.05$. Also, $n-1=15$. Therefore:

$$t_{n-1}^{\alpha/2}=t_{15}^{0.05}=1.753$$

Resulting in:

$$P(0.91m<\Delta z\leq 1.70m)=0.90$$

The above interval of values is acceptable for research, as each floor has a nominal height of 3.5m (from the confidence interval max = 1.70m <½ of 3.5m), i.e. such floor cannot be excluded from calculations. The creation of DTM follows by utilizing strategies of buildings removal and keeping the altitudes of the ground surface (Xu et al., 2008; Stournara et al., 2015) (Figure 8). The DSM and DTM were transformed in shapefile (or shp file) in the same software. The process was completed by the production of the ortho satellite image within the limits of the municipality, with a spatial resolution of 1m (Figure 10).

Figure 10: *Ortho satellite image Ikonos-2, 1: B, 2:G, 3:NIR, within the limits of the municipality of Thessaloniki. with dotted line is the historic center of the city, which was excluded by the research*

5.2. Buildings Identification-Supervised Classification

Supervised classification in Erdas Imagine 2011® was undertaken (Figure 11) on the generated ortho image within the limits of the municipality. A total of 27 classes of covers were used (11 buildings classes, 6 road classes, 4 land classes, 4 urban green classes, 1 class for shadow, and 1 class for water). The result on the accuracy of the classification is: Classification accuracy 81.58%, Kappa Statistics = 0.8118 (Masek et al., 2000; Ward et al., 2000; Zhang et al., 2002; Xian and Crane, 2005; Yuan et al., 2005; Lu and Weng, 2005; Xu, 2007; Lee et al., 2010; Ukwattage and Dayawansa, 2012). The outlines of the buildings were converted into shp file in the same software.

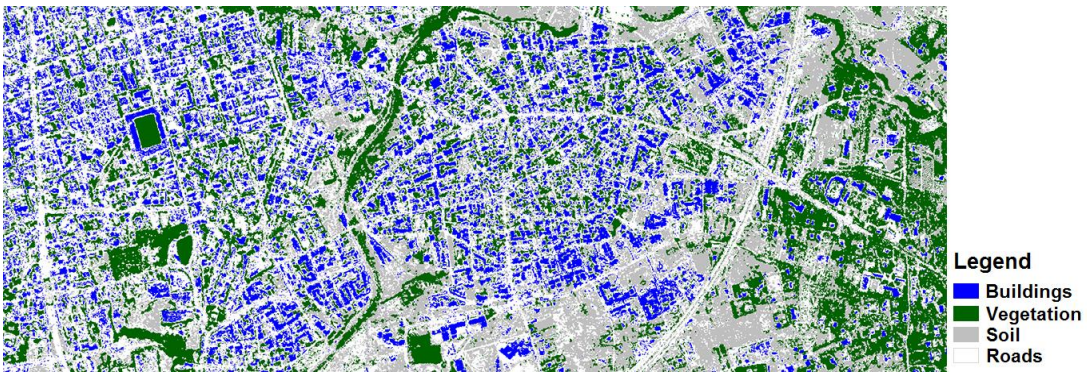

Figure 11: *Abstract from the supervised classification. In blue color are the buildings, in white the roads, in gray the soil and in green the vegetation*

6. Import of Remote Sensing Products in GIS, and Population Estimation

The shp files of the DSM, DTM and outlines of the buildings were imported in ArcMap®. In about 70% the separation of the adjacent buildings of the same kind was not allowed. For example, two buildings that are in contact and have the same shell coverage appeared as a single building in the final shp file. Such buildings may actually have different number of floors, therefore, could not be used to estimate

the population. Moreover, many roofs have different shell coverages, which also do not allow the accurate demarcation of the building plans. Finally, false detections of buildings and / or buildings that were not identified by the classification were spotted. Therefore, 85% (approximately) of the buildings of the study area were re-digitized in GIS with the help of ortho image (Figure 10). Then, purely public services, education, health, shopping malls, etc. were removed, keeping only the structures which are inhabited. The creation of the dynamic estimation model for the Number of Floors of the Building (NFB) for each building of the municipality of Thessaloniki is the next step (Figure 12).

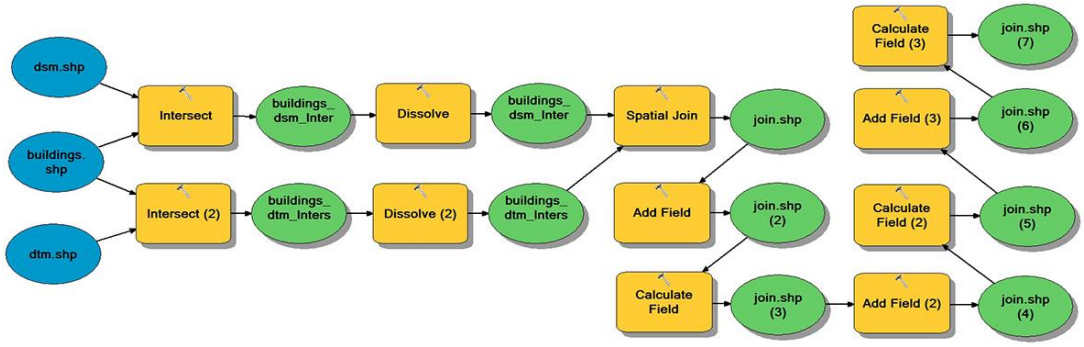

Figure 12: *Estimation model for the Number of Floors of the Building (NFB)*

According to the model, initially the intersection (Figure 12: Intersect, Figure 13c) of each building (Figure 13b) with DSM polygons (Figure 13a) is calculated. So each building now consists of all contiguous polygons (Figure 13c), each having the same or different altitude with the rest. Then, all polygons of each building are consolidated (Figure 12: Dissolve, Figure 13d), thereby yielding the border, while the total altitude of the original polygons is selected and the highest altitude of the building is maintained. The same procedure is conducted for the DTM, while, at the end, from all altitudes of the original polygons the smallest is selected and maintained for the building. Afterwards, the two new shp files are joined (Figure 12: Spatial Join) so as to produce a building file that contains the lowest and the highest altitude of each building. A new field (area, Figure 12: Add Field, join.shp (2)) is then created for the calculation of each building's area (Figure 12: Calculate Field, join.shp (3)), and a new field (NFB) for the estimation of the number of floors of each building (Figure 12: Add Field (2), join.shp (4), Calculate Field (2), join.shp (5)). At this point the results of NBF might be decimal numbers, and this is due to the estimation error of altitude differences which was described in preceding paragraphs. However, as already described, it is impossible to erase a floor. These errors can lead to decimal numbers of floors, which can then yield integers floors, if they are rounded to the nearest integer (eg NFB = 4.65 -> NFB true = 5 or NFB = 6.35 -> NFB true = 6). For this reason another field (NFB true) was created for the calculation of integer number of the floors of each building (Figure 12: Add Field (3), join.shp (6), Calculate Field (3), join.shp (7)).

The export of the attribute table of the shp file of buildings (including NFB true field) to excel followed, where the calculation of the population utilizing estimation equation (2) was performed. Rounding of the each building's population to the nearest integer was carried out (eg if the estimated population of the building is 21.12 then the final value is 21 or if the population is estimated up to 45.78 then the final value is 46), and the procedure lead to the value of 301,814. The difference from 2001 census (population 310,970) is 2.94%.

Additionally, new additional information can be drawn (Table 4). The structured surface of 20.601 buildings of the Municipality of Thessaloniki (apart from the historic center) is 3.66 km^2. The total volume of constructions is 75,297,940 m^3. Finally, maps on the number of floors and the population per building (Figure 14 and 15 respectively) of the municipality of Thessaloniki (excluding the historical center) were created.

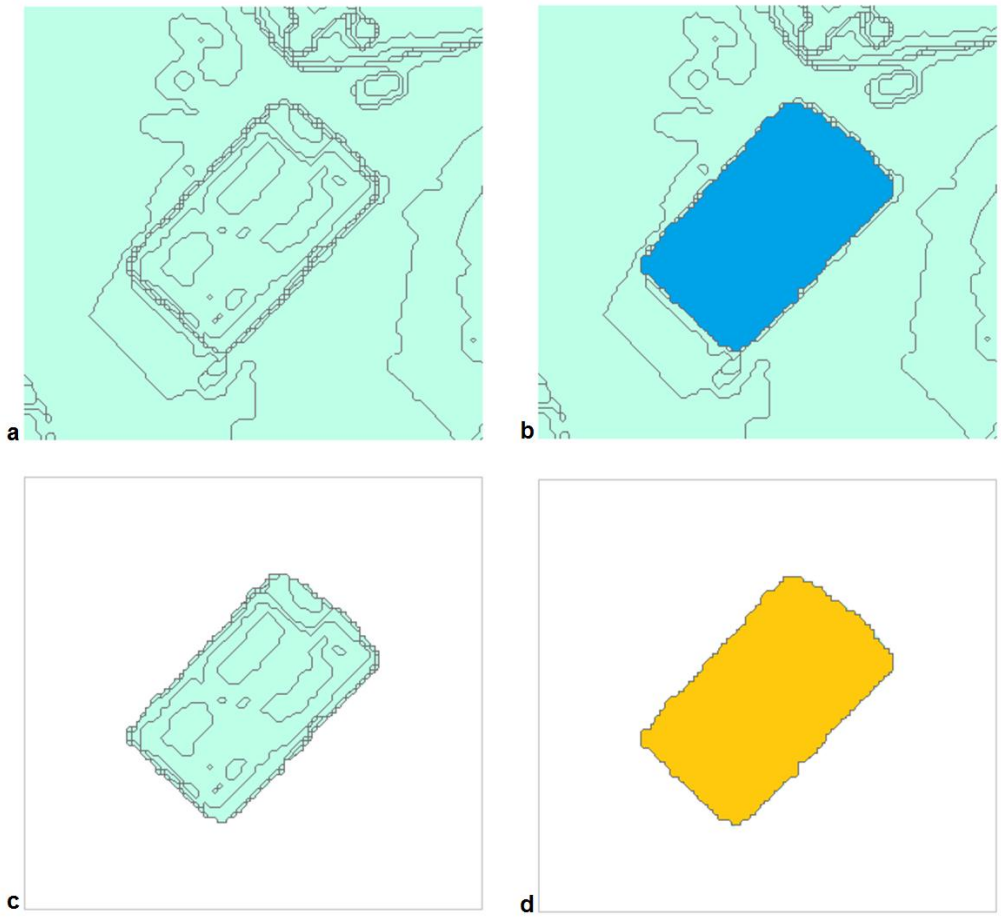

Figure 13: *a. Polygons of DSM, b. the overlay of the building, c. the intersection of the building with the DSM (the building consists of contiguous polygons), and d. polygon outline of the building by keeping the higher altitude*

Table 4: *The distribution (percentages) of floors over buildings of the Municipality of Thessaloniki (apart from the historic center)*

Floor	Percentages of buildings with respective floors
Ground floor	3.90 %
2-storey	6.00 %
3-storey	9.81 %
4-storey	9.17 %
5-storey	26.32 %
6-storey	18.85 %
7-storey	18.11 %
8-storey	4.76 %
9-storey	3.02 %
10-storey	0.05 %
12-storey	0.01 %

Figure 14: *Abstract of the study area. Number of floors per building*

Figure 15: *Abstract of the study area. Population per building*

7. Conclusions

Studies on population estimation with geoinformatics tools date back to the early 70s. Among all developed methodological approaches up to date, those that are based on high resolution satellite image processing, in combination with statistical analysis of remote sensing products, as geographically weighted regression (GWR), usually provide better results. Errors occur when building altitudes are disregarded, a fact that is treated nowadays by the use of high resolution Lidar data. However, due to the cost of Lidar data, the study proposes and demonstrates that the use of modern stereo satellite images of high spatial resolution (lower cost) results in high-precision buildings' altitude data, apart from their automated extraction of their building plans through classification.

This study takes place in the city of Thessaloniki, within the limits of its municipality. Its historic center is excluded due to its almost total commercial use of buildings.

Stereoscopic satellite images of high spatial resolution Ikonos-2 processing, led to the calculation of buildings altitudes with accuracy between 0.91m to 1.70m, an interval which is considered satisfactory

as it marginally does not allow the exclusion of one floor (standard floor height 3.5m). Also, the produced ortho image of the study area has horizontal accuracy of about 1.35m.

Supervised classification was conducted on the ortho satellite image to identify and extraction of the building plans. Where the detection and / or the extraction of the building plans were incorrect, they were extracted manually in GIS.

GIS is a valuable tool for processing and analyzing of remote sensing products, modeling the procedures for the assessment of the population, and presentation of research results. Utilizing the above remote sensing products and the empirical equation developed to calculate population per building, the estimation of the population for the municipality of Thessaloniki reaches 97.06%.

The following research refers to tests on the estimation of the population on block level in city areas with different population density, and in areas with mixed use (commercial and residential). Tests on population change as a function of value changes of the coefficients of the empirical equation will be conducted as well.

References

Al-Garni, A.M. *Mathematical Predictive Models for Population Estimation in Urban Areas using Space Products and GIS Technology.* Mathematical and Computer Modeling. 1995. 22; 95-107.

Anderson, J.S., Tuttle, B.T., Powell, R.I., and Sutton, C.P. *Characterizing Relationships between Population Density and Nighttime Imagery for Denver, Colorado: Issues of Scale and Representation.* International Journal of Remote Sensing. 2010. 31 (21) 5733-5746.

Aubrecht, C., Steinnocher, K., Hollaus, M., and Wagner, W. *Integrating Earth Observation and GIScience for High Resolution Spatial and Functional Modeling of Urban Land Use.* Computers, Environment and Urban Systems. 2009. 33; 15-25.

Avelar, S., Zah, R., and Tavares-Correa, C. *Linking Socioeconomic Classes and Land Cover Data in Lima, Peru: Assessment Through the Application of Remote Sensing and GIS.* International Journal of Applied Earth Observation and Geoinformation. 2009. 11; 27-37.

Azar, D., Graesser, J., Engstrom, R., Comenetz, J., Leddy, R.M., Schechtman, N.G., and Andrews, T. *Spatial Refinement of Census Population Distribution using Remotely Sensed Estimates of Impervious Surfaces in Haiti.* International Journal of Remote Sensing. 2010. 31 (21) 5635-5655.

Bagan, Yamagata. *Analysis of Urban Growth and Estimating Population Density using Satellite Images of Nighttime Lights and Land-Use and Population Data.* GISRS. 2015. 52; 765-780.

Benn, H., 1995: *TCRP Synthesis of Transit Practice 10: Bus Route Evaluation Standards*. Technical Report, Transportation Research Board, National Research Council, Washington, DC.

Chand, T.R.K., Badarinath, S.V.K., Elvidge, D.C., and Tuttle, T.B. *Spatial Characterization of Electrical Power Consumption Patterns over India using Temporal DMSPOLS Night-Time Satellite Data*. International Journal of Remote Sensing. 2009. 30: 647-661.

Chen, Y., Su, W., Li, J., and Sun, Z. *Hierarchical Object Oriented Classification using Very High Resolution Imagery and LiDAR Data Over Urban Areas.* Advances in Space Research. 2009. 43; 1101-1110.

Deng, C., Wu, C., and Wang, L. *Improving the Housing-Unit Method for Small-Area Population Estimation Using Remote-Sensing and GIS Information.* International Journal of Remote Sensing. 2010. 31 (21) 5673-5688.

Doll, N.H.C., 2008: *CIESIN Thematic Guide to Night-Time Light Remote Sensing and Its Applications.* Available online at: http://sedac.ciesin.columbia.edu/binaries/web/sedac/thematic-guides/ciesin_nl_tg.pdf.

Dong, P., Ramesh, S., and Nepali, A. *Evaluation of Small-Area Population Estimation using LiDAR, Landsat TM and Parcel Data.* International Journal of Remote Sensing. 2010. 31 (21) 5571-5586.

Harvey, J.K. *Population Estimation Models Based on Individual TM Pixels*. Photogrammetric Engineering and Remote Sensing. 2002. 68; 1181-1192.

Iisaka, J. and Hegedus, E. *Population Estimation from Landsat Imagery*. Remote Sensing of Environment. 1982. 12; 259-272.

Joseph et al. *Using Landsat Imagery and Census Data for Urban Population Density Modeling in Port-au-Prince, Haiti*. GISRS. 2012. 49; 228-250.

Kim, H. and Yao, X. *Pycnophylactic Interpolation Revisited: Integration with the Dasymetric-Mapping Method.* International Journal of Remote Sensing. 2010. 31 (21) 5657-5671.

Lang, S., Tiede, D., Holbling, D., Fureder, P., and Zeil, P. *Earth Observation (EO)-based Ex Post Assessment of Internally Displaced Person (IDP) Camp Evolution and Population Dynamics in Zam Zam, Darfur.* International Journal of Remote Sensing. 2010. 31 (21) 5709-5731.

Langford, M. *Obtaining Population Estimates in Non-Census Reporting Zones: An Evaluation of the 3-Class Dasymetric Method.* Computers, Environment and Urban Systems. 2006. 30; 161-180.

Lee, A.J., Lee, S.S., and Chi, K.H., 2010: *Development of an Urban Classification Method using A Built-Up Index.* Selected Topics in Power Systems and Remote Sensing, Japan. 39-43.

Li, G. and Weng, O. *Using Landsat ETM Imagery to Measure Population Density in Indianapolis, Indiana, USA*. Photogrammetric Engineering & Remote Sensing. 2005. 71 (8) 947-958.

Liu, X., 2003: *Estimation of the Spatial Distribution of Urban Population using High Spatial Resolution Satellite Imagery.* PhD Thesis, University of California, Santa Barbara, CA.

Lo, C.P., 1986: *Accuracy of Population Estimation from Medium-Scale Aerial Photography.* In American Congress on Surveying and Mapping and American Society for Photogrammetry and Remote Sensing, Falls Church, VA. 1-10.

Lo, C.P. *Automated Population and Dwelling Unit Estimation from High-Resolution Satellite Images: a GIS Approach*. International Journal of Remote Sensing. 1995. 16: 17-34.

Lo, C.P. *Population Estimation using Geographically Weighted Regression*. GIScience and Remote Sensing. 2008. 45; 131-148.

Lu, D. and Weng Q. *Urban Classification Using Full Spectral Information of Landsat ETM+ Imagery in Marion County, Indiana.* Photogrammetric Engineering & Remote Sensing. 2005. 71 (11) 1275-1284.

Lu, D., Weng, Q., and Li, G. *Residential Population Estimation using a Remote Sensing Derived Impervious Surface Approach.* International Journal of Remote Sensing. 2006. 27; 3553-3570.

Lu, Z., Im, J., Quackenbush, L., and Halligan, K. *Population Estimation Based On Multi-Sensor Data Fusion.* International Journal of Remote Sensing. 2010. 31 (21) 5587-5604.

Masek, J.G., Lindsay, E.F., and Goward, N.S. *Dynamics of Urban Growth in the Washington DC Metropolitan Area, 1973-1996, from Landsat Observations*. International Journal of Remote Sensing. 2000. 21; 3473-3486.

Mennis, J. and Hultgren, T. *Intelligent Dasymetric Mapping and Its Application to Areal Interpolation*. Cartography and Geographic Information Science. 2006. 33; 179-194.

Mao et al. *Using Land Use Data to Estimate the Population Distribution of China in 2000.* GISRS. 2012. 49; 822-853.

Qiu, F., Woller, K.L., and Briggs, R. *Modeling Urban Population Growth from Remotely Sensed Imagery and TIGER GIS Road Data*. Photogrammetric Engineering & Remote Sensing. 2003. 69 (9) 1031-1042.

Shuo-sheng, W., Xiaomin, Q., and Wang, Le. *Population Estimation Methods in GIS and Remote Sensing: A Review.* GIScience and Remote Sensing. 2005. 42 (1) 58-74.

Silvan-Cardenas, L.J., Wang, L., Rogerson, P., Wu, C., Feng, T., and Kamphaus, D.B. *Assessing Fine-Spatial-Resolution Remote Sensing For Small-Area Population Estimation.* International Journal of Remote Sensing. 2010. 31 (21) 5605-5634.

Smith, S., and Mandell, M. *A Comparison of Population Estimation Methods: Housing Unit versus Component II, Ratio Correlation, and Administrative Records*. Journal of the American Statistical Association. 1984. 79 (386) 282-289.

Smith, S., Nogle, J., and Cody, S. *A Regression Approach to Estimating the Average Number of Persons per Household.* Demography. 2002. 39; 697-712.

Stournara, P., Georgiadis, C., Kaimaris, D., Tsakiri-Strati, M., and Tsioukas, V., 2015: *Feature Extraction from Geoeye-1 Stereo Pairs Data for Forested Area.* In Proceedings the 36th International Symposium on Remote Sensing of Environment, Berlin, Germany, ISRSE36-67-2.

Sutton, P.C. *Modeling Population Density Using Nighttime Satellite Imagery and GIS.* Computers, Environment and Urban Systems. 1997. 21; 227-244.

Sutton, P.C. *An Empirical Environmental Sustainability Index Derived Solely from Nighttime Satellite Imagery and Ecosystem Service Values*. Population and Environment. 2003. 24; 293-312.

Tatem, A.J., Noor, M.A., Vonhagen, C., Digregorio, A., and Hay, S. *High Resolution Population Maps For Low Income Nations: Combining Land Cover and Census in East Africa.* PloS ONE. 2007. 2; e 1298.

Ukwattage, L.N. and Dayawansa, N.D.K. *Urban Heat Islands and the Energy Demand: An Analysis for Colombo City of Sri Lanka Using Thermal Remote Sensing Data.* International Journal of Remote Sensing and GIS. 2012. 1 (2) 124-131.

Ward, D., Phinn, S.R., and Murray, A.T. *Monitoring Growth in Rapidly Urbanizing Areas Using Remotely Sensed Data.* Professional Geographers. 2000. 52 (3) 371-386.

Wu, C. and Murray, T.A. Population Estimation using Landsat Enhanced Thematic Mapper Imagery. Geographical Analysis. 2007. 39; 26-43.

Wu, S., Wang, L., and Qiu, X. *Incorporating GIS Building Data and Census Housing Statistics for Sub-Block-Level Population Estimation.* The Professional Geographer. 2008. 60; 121-135.

Xian, G. and Crane, M. *Assessment of Urban Growth in the Tampa Bay Watershed using Remote Sensing Data*. Remote Sensing of Environment. 2005. 97 (2) 203-205.

Xie, Z., Roberts, C., and Johnson, B. *Object-based Target Search using Remotely Sensed Data: A Case Study in Detecting Invasive Exotic Australian Pine in south Florida.* ISPRS Journal of Photogrammetry and Remote Sensing. 2008. 63; 647-660.

Xu, F., Woodhouse, N., Xu, Z., Marr, D., Yang, X., and Wang, Y. *Blunder Elimination Techniques in Adaptive Automatic Terrain Extraction.* The International Archives of the Photogrammetry, Remote Sensing and Spatial Information Sciences. 2008. Vol. XXXVII. Part B1. Beijing.

Xu, H. *Extraction of Urban Built-up Land Features from Landsat Imagery Using a Thematic-oriented Index Combination Technique.* Photogrammetric Engineering & Remote Sensing. 2007. 73 (12) 1381-1391.

Yagoub, M.M. *Application of Remote Sensing and Geographic Information Systems (GIS) to Population Studies in the Gulf: A Case of Al Ain City (UAE).* Journal of the Indian Society of Remote Sensing. 2006. 34 (1) 7-21.

Yuan, F., Sawaya, K.E., Loeffelholz, B.C., and Bauer, M.E. *Land Cover Classification and Change Analysis of the Twin Cities (Minnesota) Metropolitan Area by Multitemporal Landsat Remote Sensing.* Remote Sensing of Environment. 2005. 98 (2-3) 317-328.

Zhang, Q., Wang, J., Peng, X., Gong, P., and Shi, P. *Urban Built-Up Land Change Detection with Road Density and Spectral Information from Multi-Temporal Landsat TM Data.* International Journal of Remote Sensing. 2002. 23 (15) 3057-3078.

Zhu, H., Li, Y., Liu, Z., and Fu, B. *Estimating The Population Distribution in a County Area in China Based on Impervious Surfaces.* Photogrammetric Engineering & Remote Sensing. 2015. 81 (2) 155-163.